

An axisymmetric limit for the width of the Hadley cell on planets with large obliquity and long seasonality

I. Guendelman¹ and Y. Kaspi¹

¹Weizmann Institute of Science, Department of Earth and Planetary Sciences, Rehovot, Israel

Key Points:

- = The Hadley cell ascending branch position in planets with strong seasonal variation of temperature is mainly bounded by the rotation rate.
- = A similar rotation rate dependence arises in the axisymmetric theory.
- = This theory can explain the ascending branch position on Mars and Titan.

arXiv:1903.11656v1 [astro-ph.EP] 27 Mar 2019

Corresponding author: Ilai Guendelman, ilai.guendelman@weizmann.ac.il

Abstract

Hadley cells dominate the meridional circulation of terrestrial atmospheres. The Solar System terrestrial atmospheres, Venus, Earth, Mars and Titan, exhibit a large variety in the strength, width and seasonality of their Hadley circulation. Despite the Hadley cell being thermally driven, in all planets, the ascending branch does not coincide with the warmest latitude, even in cases with very long seasonality (e.g., Titan) or very small thermal inertia (e.g., Mars). In order to understand the characteristics of the Hadley circulation in case of extreme planetary characteristics, we show both theoretically, using axisymmetric theory, and numerically, using a set of idealized GCM simulations, that the thermal Rossby number dictates the character of the circulation. Given the possible variation of thermal Rossby number parameters, the rotation rate is found to be the most critical factor controlling the circulation characteristics. The results also explain the location of the ascending branch on Mars and Titan.

1 Introduction

Observations and models show that the Hadley circulation varies considerably between the Solar System terrestrial atmospheres of Venus, Earth, Mars and Titan. Venus' lower atmosphere is composed of two hemispherically symmetric equator-to-pole Hadley cells [Read, 2013; Sánchez-Lavega *et al.*, 2017]. On Earth, similar to Venus, Hadley cells exist in both hemispheres, but due to Earth's obliquity, the ascending branch latitude and the strength of the two cells vary seasonally, where during the solstice there is a strong and wide winter cell and a narrow and weak summer cell [e.g., Dima and Wallace, 2003].

Both Mars and Titan, exhibit stronger seasonality in the Hadley circulation compared to Earth, despite the fact that the obliquity of Mars and Titan is similar to Earth's obliquity. The strong seasonality on Mars is due to its thin atmosphere and rocky surface resulting in a low thermal inertia and a short radiative timescale. Mars' Hadley circulation transits from two hemispherically symmetric cells at equinox, to one solstice cell, with air rising at midlatitudes [Read *et al.*, 2015]. Thus, although at solstice, Mars' maximum surface temperature is at the pole, the Hadley cell ascending branch does not reach the pole.

Titan's tropospheric radiative timescale is considerably longer than its orbital period [Mitchell and Lora, 2016], which explains why Titan's maximum surface temper-

ature seem to stay near the equator during the seasonal cycle [Jennings *et al.*, 2016; Lora *et al.*, 2015]. However, observations of Titan’s methane clouds, show a significant seasonal cycle as they shift from one pole to the other during Titan’s year [Brown *et al.*, 2002; Turtle *et al.*, 2011; Roe, 2012; Turtle *et al.*, 2018]. Different models associate the polar clouds to different phenomena. Schneider *et al.* [2012] associate the polar clouds to the meridional convergence (analogous to the inter tropical convergence zone, ITCZ, on Earth) indicating a pole-to-pole Hadley circulation [e.g., Roe, 2012]. In contrast, Lora *et al.* [2015] and other studies [e.g., Mitchell *et al.*, 2006, 2009; Mitchell, 2008; Newman *et al.*, 2016] relate the polar clouds to intensive polar warming during solstice, while the meridional convergence occurs at midlatitudes.

The variability of the terrestrial atmospheric circulation within the Solar System, is a result of the variability in the planets’ orbit, rotation rate, atmospheric mass, radius etc. Different studies explored the effect of different planetary parameters on the atmospheric circulation, showing that the large scale circulation depends greatly on the planetary parameters and atmospheric characteristics [e.g., Ferreira *et al.*, 2014; Kaspi and Showman, 2015; Linsenmeier *et al.*, 2015; Faulk *et al.*, 2017; Chemke and Kaspi, 2017].

More specifically, Faulk *et al.* [2017] studied the dependence of the meridional circulation seasonal cycle on the rotation rate using an idealized aquaplanet GCM, showing that in the case of an Earth-like rotation rate, the ITCZ and the ascending branch of the Hadley circulation do not reach the pole, even in an eternal solstice case, where the maximum temperature is at the pole. This result, together with Mars’ ascending branch not reaching the pole, even though its maximal surface temperature is at the pole [Forget *et al.*, 1999; Read *et al.*, 2015] and some Titan models predicting the ascending branch being poleward from the warmest latitude [e.g., Lora *et al.*, 2015], is puzzling. Theoretical expectations are that the Hadley cell ascending branch, being a thermally driven circulation, will follow the warmest latitude [Neelin and Held, 1987], or the latitude of maximum low level moist static energy [Emanuel *et al.*, 1994; Privé and Plumb, 2007], which is not the case for Mars and neither for the Faulk *et al.* [2017] simulations. This study shows that axisymmetric theory [Held and Hou, 1980; Lindzen and Hou, 1988; Caballero *et al.*, 2008] has a similar rotation rate dependence as the modeling results and the observations on Mars and Titan show.

For Earth, there are several other theories regarding the Hadley circulation and the ITCZ position, that unlike the axisymmetric theory take into account the eddy contribution, and involve processes such as the flux of eddies across the equator [e.g., *Kang et al.*, 2008; *Bischoff and Schneider*, 2014; *Adam et al.*, 2016a,b; *Wei and Bordoni*, 2018], moist processes [e.g., *Neelin and Held*, 1987], baroclinicity [*Held*, 2000] and supercriticality [*Korty and Schneider*, 2008; *Levine and Schneider*, 2015]. However, in this study which aims to understand the leading order effects over a wide range of conditions, we focus on the simpler, axisymmetric theory, as a leading order theory for the zonally symmetric climate balance. In section 2 we derive the axisymmetric theory for the solstice case following *Lindzen and Hou* [1988] (hereafter LH88), and solve it numerically to include a wide range of planetary parameters. In section 3 we briefly describe the numerical model and present the simulation results, relating them to the axisymmetric theory. In section 4 we discuss the results and their implication for the Solar System atmospheres.

2 Axisymmetric theory

The axisymmetric theory introduced by *Held and Hou* [1980] and further developed by LH88 to include the solstice case, is a theory for the Hadley circulation that neglects eddy contribution and diffusive processes. Despite the importance of eddies [e.g., *Walker and Schneider*, 2006], the axisymmetric theory has been found to overall give a good leading order estimate to the cell extent. Following LH88, angular momentum conservation at the top of the cell is assumed, and the angular momentum conserving wind, at latitude ϕ , of an air parcel starting at rest from latitude ϕ_1 (the ascending branch of the Hadley cell) is

$$u_M = \Omega a \frac{\cos^2 \phi_1 - \cos^2 \phi}{\cos \phi}, \quad (1)$$

where Ω is the planetary rotation rate and a is the planetary radius. Assuming that the flow is in cyclostrophic balance and that thermal wind balance holds to leading order, Eq. 1 together with hydrostatic balance, results in an expression for the angular momentum conserving potential temperature (θ)

$$\frac{\theta(\phi) - \theta(\phi_1)}{\theta_0} = -\frac{\Omega^2 a^2 (\sin^2 \phi - \sin^2 \phi_1)^2}{2gH \cos^2 \phi}, \quad (2)$$

where θ_0 is some reference potential temperature and H is the troposphere height. Equation 2 can be expressed using the thermal Rossby number $R_t = \frac{2gH\Delta\theta}{\Omega^2 a^2}$ [*Held and Hou*,

1980] to give

$$\frac{\theta(\phi) - \theta(\phi_1)}{\theta_0} = -\frac{\Delta_H (\sin^2 \phi - \sin^2 \phi_1)^2}{R_t \cos^2 \phi}, \quad (3)$$

where Δ_H is the meridional fractional change of the radiative equilibrium temperature (LH88 and Eq. 4). Taking a small angle approximation, the width of the circulation in the equinox case is $\propto R_t^{1/2}$ [Held and Hou, 1980] and for the solstice case $\propto R_t^{1/3}$ [Caballero et al., 2008].

In order to find the Hadley circulation edges, namely, the latitudes of the ascending and descending branches, we assume that the cells are energetically closed, that the temperature at the edge of the cells is continuous and that outside of the Hadley circulation the temperature is a radiative equilibrium temperature θ_e

$$\frac{\theta_e}{\theta_0} = 1 + \frac{\Delta_H}{3}(1 - 3(\sin \phi - \sin \phi_0)^2), \quad (4)$$

where ϕ_0 is the latitude of maximum θ_e . The energetically closed cell and temperature continuity assumptions translate to the following set of equations

$$\int_{\phi_w}^{\phi_1} (\theta - \theta_e) \cos \phi d\phi = 0, \quad (5)$$

$$\int_{\phi_1}^{\phi_s} (\theta - \theta_e) \cos \phi d\phi = 0, \quad (6)$$

$$\theta(\phi_1) = \theta_e(\phi_1), \quad (7)$$

$$\theta(\phi_w) = \theta_e(\phi_w), \quad (8)$$

$$\theta(\phi_s) = \theta_e(\phi_s), \quad (9)$$

where ϕ_s and ϕ_w are the latitudes of the Hadley cell descending branch in the summer and winter hemispheres (edges of the circulation), respectively. The unknowns that equations (5)-(9) solve for are the ascending and descending branches latitudes ϕ_1 , ϕ_s , ϕ_w and the temperature at the ascending branch $\theta(\phi_1)$. Graphically, the energetically closed cell assumption translates to an equal area between the angular momentum conserving and the radiative equilibrium temperature curves inside each cell. Figure 1 depicts the angular momentum conserving (dashed) and the radiative equilibrium (solid) temperature curves, multiplied by $\cos \phi$ for different cases, depicting the closed cell argument. Figures 1a and 1c are similar to Figure 5 in LH88 with the difference that here θ and θ_e are multiplied by $\cos \phi$, as the small angle approximation is not appropriate in this case. Fig. 1a shows the hemispherically symmetric cell and Fig. 1c shows the $\phi_0 = 6^\circ$ case, representing an Earth-like scenario. Figures 1b and 1d are for different temperature gradients and different rotation rates, respectively, where the latitude of maximum

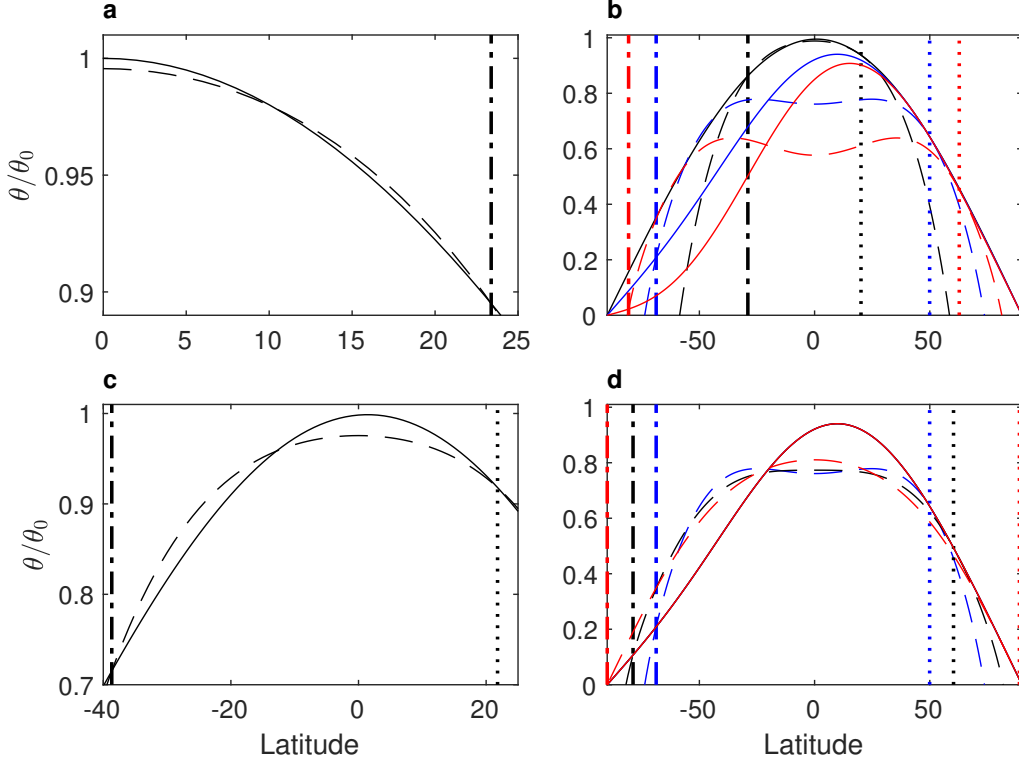


Figure 1. The radiative equilibrium potential temperature and the angular momentum temperature both multiplied by cosine of latitude ($\theta_e \cos \phi / \theta_0$, solid, and $\theta \cos \phi / \theta_0$, dashed, respectively), and normalized by maximum θ_e / θ_0 . The vertical dotted and dashed dotted lines are for the winter cell ascending and descending branches, respectively. Panels a and c are similar to Fig. 5 in LH88, where panel a is the solution for the hemispherically symmetric case ($\phi_0 = 0^\circ$), and panel c is the solution for $\phi_0 = 6^\circ$ with $\Delta_H = 1/6$ and Earth-like rotation rate. In panels b and d, $\phi_0 = 45^\circ$, where in panel b each color represents a different value of Δ_H with the values 0.01 (black), 1/6 (blue) and 1/3 (red), all with Earth-like rotation rate. Panel d shows the solutions for different rotation rates, 0.5 (red) 0.75 (black) and 1 (blue) all in Earth rotation rate units, with $\Delta_H = 1/6$.

radiative temperature is at latitude 45° . All plots in Fig. 1 show the position of the winter cell ascending (dotted line) and descending (dashed-dotted line) branches. Only the winter cell is shown, as for strong seasonal cases, which are the focus of this study, a summer cell barely exists. Comparing between Figures 1b and 1d, shows that slowing down the rotation rate is more efficient in widening the circulation than increasing the temperature gradient.

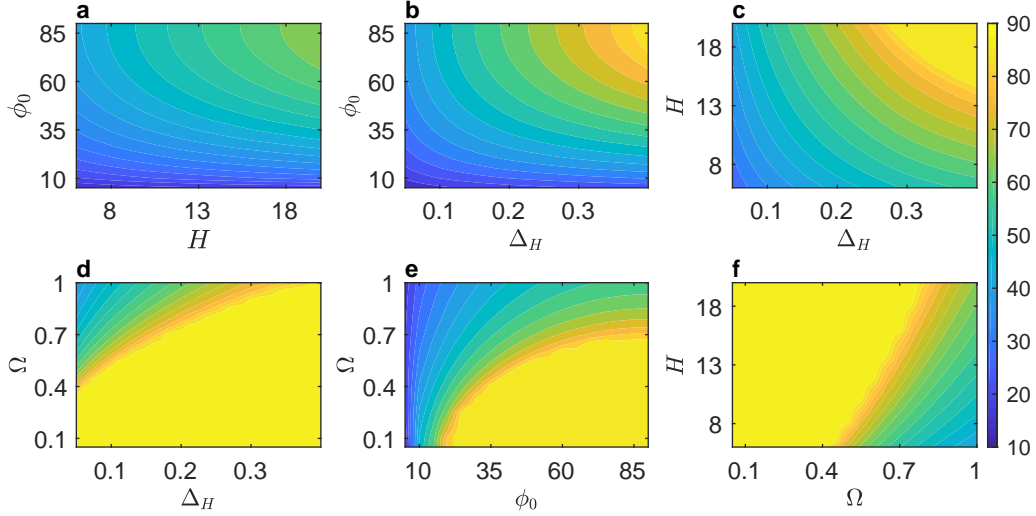


Figure 2. Axisymmetric solutions for the ascending branch latitude (color), in the parameter space of ϕ_0 , Δ_H , H , and Ω . The parameters are ϕ_0 , the latitude of maximum radiative equilibrium temperature, ranging from 5° to 90° , with a value of 90° when kept constant. The meridional radiative equilibrium temperature gradient, Δ_H , ranging from 0.01 to 0.4, with a value of 0.17 when kept constant. The tropopause height, H , ranging from 6 to 20 km, with a value of 15 km when kept constant. The rotation rate, Ω , ranging from 0.05 to 1 in Earth’s rotation rate units, with a value of 1 when kept constant.

The axisymmetric theory solutions shown in Figure 1 together with equations (2) and (4), show that the latitudes of the ascending and descending branches depend on different parameters. Solving numerically equations (5)-(9) for a wide range of Ω , Δ_H , ϕ_0 and H values (Fig. 2) shows a clear difference between cases where the rotation rate is slowed down (Fig. 2d-f), where the ascending branch easily reaches the pole, and cases where the rotation rate is kept with an Earth-like value (Fig. 2a-c). This demonstrates that an Earth-like rotation rate or faster, limits the expansion of the circulation, such that even if ϕ_0 is at the pole, and, for example, Δ_H is increased (over a realistic range), it is unlikely for ϕ_1 to reach the pole unless the rotation rate is slowed down. This result is consistent with the simulations of *Faulk et al.* [2017]. The choice of parameter values is guided by the observed values in the Solar System. Δ_H , the normalized horizontal temperature difference, gets its largest value for Mars [~ 0.4 , e.g., *Read et al.*, 2015], and lowest value for Venus [with nearly zero temperature gradient, e.g., *Read*, 2013]. The tropopause height, H , taken to be the circulation height scale [*Walker and Schnei-*

der, 2006], is highest on Titan and Mars reaching to ~ 20 km [e.g. *Read et al.*, 2015; *Lora et al.*, 2015].

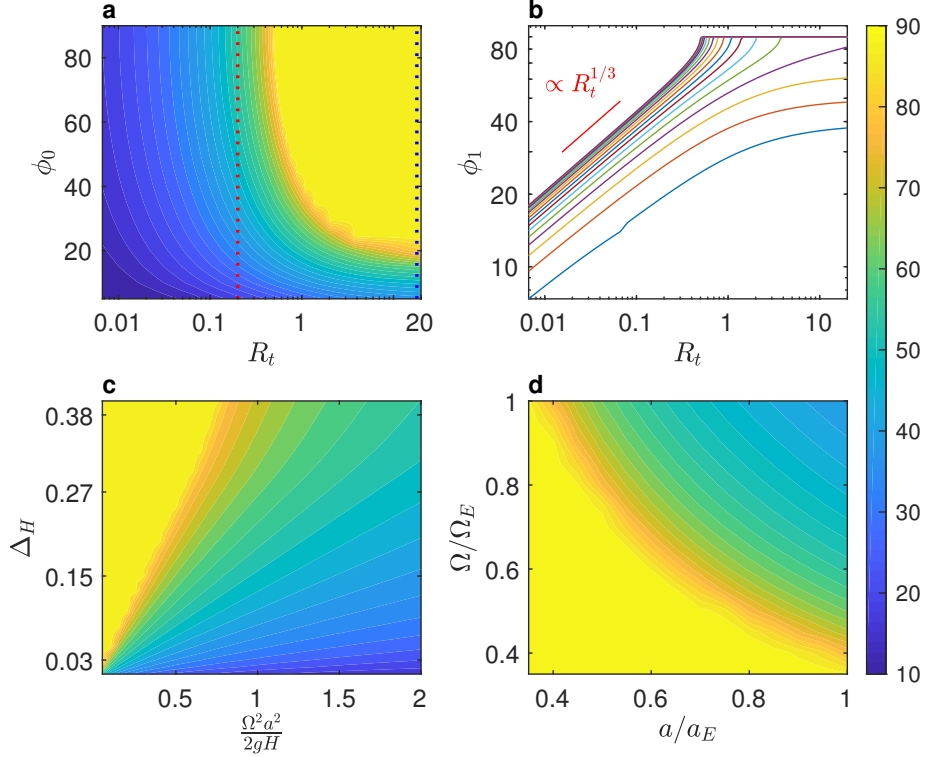


Figure 3. The latitude of ascending branch as a function of ϕ_0 , the thermal Rossby number, R_t , and its decomposition. (a) The ascending branch as a function of ϕ_0 and R_t , where the dotted blue and red lines represent the R_t value of Titan and Mars, respectively. Each curve in (b) is for a different ϕ_0 value ranging from 90° (top) to 5° (bottom) in a log-log plot of ϕ_1 as a function of R_t , showing the correspondence to the *Caballero et al.* [2008] scaling. (c) and (d) are the ascending branch latitude (color) as a function of $\frac{\Omega^2 a^2}{2gH}$ and Δ_H and for different values of a and Ω , respectively, where a_E and Ω_E are Earth’s radius and rotation rate. In (c) $g = 3 \text{ ms}^{-2}$ is used, which is between the Mars and Titan surface gravity values.

In order to understand this rotation rate dependence, we plot the ascending branch latitude as a function of R_t and ϕ_0 (Fig. 3a), showing that for each value of ϕ_0 the position of the ascending branch is strongly dependent on R_t (Fig. 3a,b). For small values of R_t there is a good agreement with the *Caballero et al.* [2008] scaling (Fig 3b). The values of R_t for the Solar System terrestrial atmospheres vary from 0.06 on Earth to 370 on Venus, with the value for Mars being 0.2 and for Titan 18 [*Read*, 2011]. Decompos-

ing R_t into $\frac{\Omega^2 a^2}{2gH}$ and Δ_H , which is a natural decomposition to a dynamical component ($\frac{\Omega^2 a^2}{2gH}$) and a radiative one (Δ_H), shows the range of possible values of $\frac{\Omega^2 a^2}{2gH}$ is larger compared to that of Δ_H (Fig 3c). As a result, this factor will have a larger role in limiting the width of the circulation. Examining the elements in $\frac{\Omega^2 a^2}{2gH}$ shows a strong dependence on the rotation rate and radius (Fig. 3d). Taking the Solar System terrestrial atmospheres as a proxy, and comparing between the range of the different parameters in R_t , shows that the rotation rate is the only parameter known to vary by two orders of magnitude (Earth and Venus), while all other parameters vary by one order of magnitude or less. This together with the strong dependence of R_t on the rotation rate is what makes the rotation rate the limiting factor on the circulation extent. Also, taking a closer look at the radius dependence, shows that it is not as strong as the rotation rate dependence, considering the surface gravity dependence on the planetary radius $g = 4\pi G\rho a/3$. Here ρ is the planet's mean density, which is a more fundamental characteristic of the planet than its surface gravity, and G is the universal gravitational constant. Therefore, a more useful form to write the thermal Rossby number in this context, is

$$R_t = \frac{8\pi\rho GH\Delta_H}{3\Omega^2 a}. \quad (10)$$

Expressing R_t in this form emphasizes the circulation dependence on the rotation rate.

3 Idealized GCM simulations

3.1 Model description

In order to test the theoretical framework presented in section 2 in a more complete model, we use an idealized moist aquaplanet GCM [Frierson *et al.*, 2006], based on the GFDL dynamical core [Anderson *et al.*, 2004], used in this context by Faulk *et al.* [2017]. The model radiation scheme is augmented to include a diurnal mean seasonal insolation dependence on obliquity [Pierrehumbert, 2010]. Similar to Faulk *et al.* [2017] the atmospheric optical depth is constant with latitude. The model solves the primitive equations with a horizontal spectral grid of $2.8^\circ \times 2.8^\circ$ (T42) and 25 uneven vertical levels. To analyze the climate we use a 50 year climatology after reaching a statistical steady state. Figure 4a shows the model results for Earth-like parameters. The model shows a generally similar climate as Earth's [Kaspi and Showman, 2015].

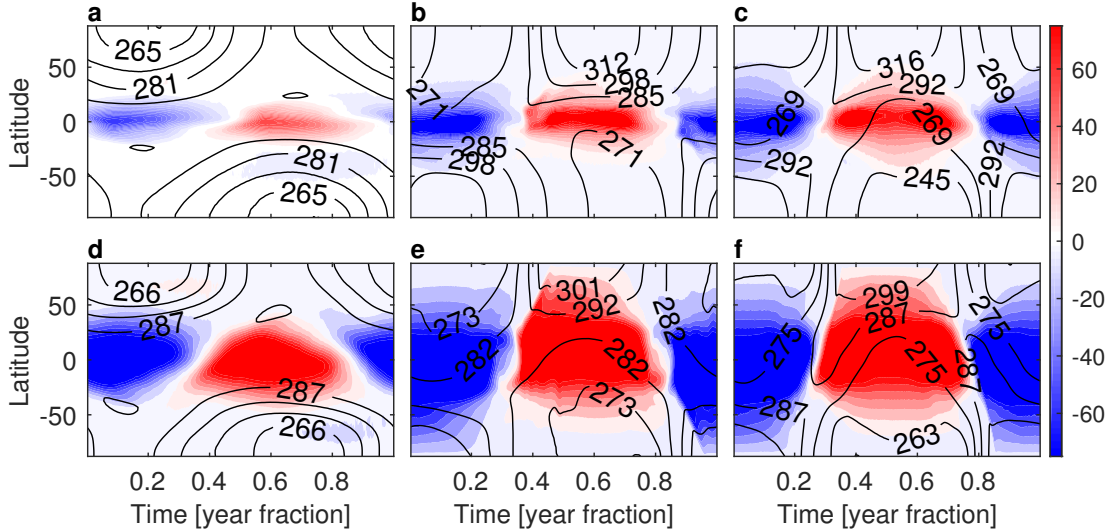


Figure 4. Hovmoller diagram of the streamfunction, $\psi = 2\pi a \int v dp/g$, where v is the zonal mean meridional wind, at its height of global maximum value (color, units $10^{10} \text{ kg s}^{-1}$) and surface temperature (contours, K) for different climates. The abscissa is a time axis, showing the year fraction. Top row simulations are with an Earth-like rotation rate and the bottom row simulations are with 1/4 of Earth’s rotation rate. (a) and (d) are Earth-like simulations with obliquity 23° and an Earth-like orbital period. (b) and (e) Simulations with obliquity 90° and an Earth-like orbital period. (c) and (f) Simulations with obliquity 90° and 4 times Earth’s orbital period.

3.2 Simulation results

Three simulations with different degree of seasonality: Earth-like, obliquity 90° with an Earth-like orbital period and obliquity 90° with four times Earth’s orbital period, are repeated with an Earth-like rotation rate and 1/4 of Earth’s rotation rate. Figures 4 and 5 show that shifting the maximal temperature poleward from a reference Earth-like state (Fig. 4a), does not result in a global pole-to-pole Hadley circulation for simulations with an Earth-like rotation rate (Fig. 4b), even when the temperature gradient is increased (Fig. 4c). However, slowing down the rotation rate, allows the ascending branch to reach the pole, similar to *Faulk et al.* [2017]. These results coincide with the theoretical solution of equations (5)-(9) (Fig. 2), where the ascending branch, for a realistic range of Δ_H , does not reach the pole for an Earth-like rotation rate.

Figure 5 shows that during the solstice of the strong seasonal cases, the meridional streamfunction follows the angular momentum contours (Fig. 5b-f), implying that the eddy contribution is small. This means that despite the importance of eddies in the more Earth-like cases for the extent of the Hadley circulation [e.g., *Walker and Schneider, 2005, 2006; Korty and Schneider, 2008*] eddies seem to play less of a role in these cases. This alignment, relates to a previously suggested regime transition between an eddy mediated circulation at equinox, to a thermally driven one at solstice, where eddies do not contribute, suggesting that the use of axisymmetric theory is appropriate [*Bordoni and Schneider, 2008, 2010; Merlis et al., 2013; Geen et al., 2018*]. Aside from the seasonal regime transition, there is a rotation rate related transition, where by slowing down the rotation rate, the streamfunction follows angular momentum contours. This regime transition in both rotation rate and seasonality is a result of weaker eddy momentum flux convergence that in turn allow the streamfunction to follow the angular momentum contours [*Faulk et al., 2017*]. Consistent with the angular momentum conserving cell these simulations do not exhibit superrotation. However, simulations with slower rotation rates (more similar to Titan and Venus) may exhibit superrotation [e.g., *Kaspi and Showman, 2015*], though the existence of superrotation together with a strong seasonal cycle is complex [*Mitchell et al., 2014*].

4 Discussion and conclusion

Previous studies showed that as a planet rotates faster, the Hadley circulation contracts, the streamfunction becomes multicellular and the number of jets increases [*Navarra and Boccaletti, 2002; Walker and Schneider, 2006; Kaspi and Showman, 2015; Chemke and Kaspi, 2015a,b*]. *Faulk et al. [2017]*, studying the effect of the rotation rate in a seasonal cycle, showed that for a planet with an Earth-like rotation rate the Hadley cell ascending branch and the latitude of the ITCZ do not reach the pole, even when the maximum surface temperature is at the pole and the seasonal cycle is very long.

Similar to *Faulk et al. [2017]*, using an idealized GCM with different degrees of seasonality we show that for Earth-like rotation rate cases the Hadley cell ascending branch does not reach the pole (Figures 4 and 5). A similar rotation rate limitation arises from the axisymmetric theory, predicting that the Hadley cell ascending branch latitude is limited for Earth-like rotation rate cases (Figure 2). This rotation rate dependence is a result of the angular momentum conservation and thermal wind assumptions that makes

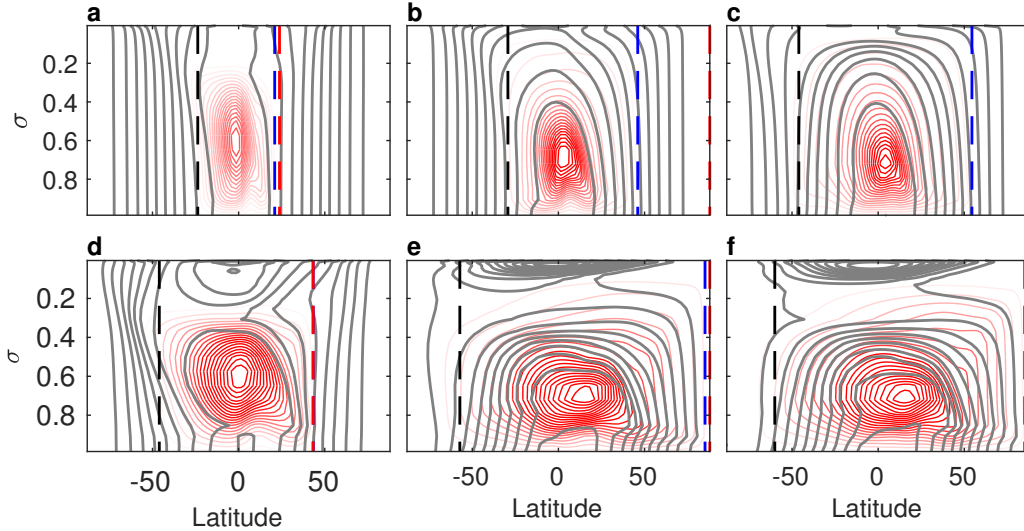


Figure 5. Streamfunction (red contours) and angular momentum (gray contours) vertical structure during southern hemisphere summer solstice, for different climates. Blue and Black vertical dashed lines are for the positions of the ascending and descending branches, respectively, defined to be the latitudes where the streamfunction reaches 5% of its maximum [Walker and Schneider, 2006; Faulk et al., 2017]. The red dashed vertical line is for the position of the maximum surface temperature. The simulation parameters for the different panels are the same as in Figure 4.

the width of the circulation to be a function of the thermal Rossby number (Figure 3). The quadratic dependence of the thermal Rossby number on the rotation rate (Eq. 10), and the limited range the other thermal Rossby number parameters exhibit in the Solar System planetary atmospheres, imply that the strongest limiting factor in controlling the ascending branch of the Hadley circulation is the rotation rate.

Studying these extreme cases, and the climate dependence on different planetary parameters, gives insight to the expected climate on other planetary atmospheres. Our Solar System terrestrial atmospheres are a good example for a variety of circulations, due to their large variability in planetary characteristics. Of particular interest is the seasonality on Mars and Titan, both exhibiting a different circulation response to the seasonally varying surface temperature [Read et al., 2015; Mitchell and Lora, 2016]. During the Martian solstice, maximum surface temperature is at the pole, however, the Hadley cell ascending branch is located at midlatitudes [Read et al., 2015], consistent with the axisymmetric theory using Mars' R_t (red dotted line in Fig. 3a).

On Titan, observational studies show that the maximum surface temperature stays around the equator during Titan’s year [Jennings *et al.*, 2016]; yet, cloud observations show a significant seasonal variation [e.g., Turtle *et al.*, 2018]. Models of Titan’s climate vary depending on their physical aspects [Hörst, 2017], with some models associating polar clouds with the Hadley cell ascending branch [e.g., Schneider *et al.*, 2012] while others locate the ascending branch at midlatitudes [e.g., Lora *et al.*, 2015]. The warmest latitude also varies between models [e.g., the difference between dry and moist cases in Newman *et al.*, 2016]. Particularly, Lora *et al.* [2015] is an interesting case, where the peak surface temperature stays close to the equator while the ascending branch is located poleward, at midlatitudes. This variety of models can be explained using the axisymmetric theory. Following the blue dotted line in Fig. 3a, which represents the R_t value of Titan, we indeed find that if ϕ_0 is taken to be $\sim 10^\circ$ the position of the ascending branch is at $\sim 45^\circ$, in a general agreement with Lora *et al.* [2015]. Also if $\phi_0 \geq 30$ the ascending branch is predicted to be at the pole, similar to the dry case in Newman *et al.* [2016].

Acknowledgments

We thank Rei Chemke for fruitful conversations and help with the model configuration. We also thank the reviewers that helped improve this manuscript. Datasets used in this manuscript is available on <https://doi.org/10.5281/zenodo.1442928>. The authors acknowledge support from the Minerva Foundation with funding from the Federal German Ministry of Education and Research, and from the Weizmann institute Helen Kimmel Center for Planetary Science.

References

- Adam, O., T. Bischoff and T. Schneider (2016), Seasonal and interannual variations of the energy flux equator and ITCZ. Part I: Zonally averaged ITCZ position, *J. Climate* 29(9) 3219–3230.
- Adam, O., T. Bischoff and T. Schneider (2016), Seasonal and interannual variations of the energy flux equator and ITCZ. Part II: Zonally varying shifts of the ITCZ, *J. Climate* 29(20) 7281–7293.
- Anderson, J. L., V. Balaji, A. J. Broccoli, W. F. Cooke, T. L. Delworth, K. W. Dixon, L. J. Donner, K. A. Dunne, S. M. Freidenreich, et al. (2004), The new GFDL global atmosphere and land model AM2-LM2: Evaluation with prescribed

- SST simulations, *J. Atmos. Sci.*, *17*(24), 4641–4673.
- Bischoff, T., and T. Schneider (2014), Energetic constraints on the position of the intertropical convergence zone, *J. Climate*, *27*(13), 4937–4951.
- Bordoni, S., and T. Schneider (2008), Monsoons as eddy-mediated regime transitions of the tropical overturning circulation, *Nature Geoscience*, *1*(8), 515.
- Bordoni, S., and T. Schneider (2010), Regime transitions of steady and time-dependent Hadley circulations: Comparison of axisymmetric and eddy-permitting simulations, *J. Atmos. Sci.*, *67*(5), 1643–1654.
- Brown, M. E., A. H. Bouchez, and C. A. Griffith (2002), Direct detection of variable tropospheric clouds near Titan’s south pole, *Nature*, *420*(6917), 795.
- Caballero, R., R. T. Pierrehumbert, and J. L. Mitchell (2008), Axisymmetric, nearly inviscid circulations in non-condensing radiative-convective atmospheres, *Q. J. R. Meteorol. Soc.*, *134*(634), 1269–1285.
- Chemke, R., and Y. Kaspi (2015a), Poleward migration of eddy-driven jets, *J. Adv. Model. Earth Syst.*, *7*(3), 1457–1471.
- Chemke, R., and Y. Kaspi (2015b), The latitudinal dependence of atmospheric jet scales and macroturbulent energy cascades, *J. Atmos. Sci.*, *72*(10), 3891–3907.
- Chemke, R., and Y. Kaspi (2017), Dynamics of massive atmospheres, *Astrophys. J.*, *845*(1), 1.
- Dima, I. M., and J. M. Wallace (2003), On the seasonality of the Hadley cell, *J. Atmos. Sci.*, *60*(12), 1522–1527.
- Emanuel, K. A., J. David Neelin, and C. S. Bretherton (1994), On large-scale circulations in convecting atmospheres, *Q. J. R. Meteorol. Soc.*, *120*(519), 1111–1143.
- Faulk, S., J. Mitchell, and S. Bordoni (2017), Effects of rotation rate and seasonal forcing on the ITCZ extent in planetary atmospheres, *J. Atmos. Sci.*, *74*(3), 665–678.
- Ferreira, D., J. Marshall, P. A. O’Gorman, and S. Seager (2014), Climate at high-obliquity, *Icarus*, *243*, 236–248.
- Forget, F., F. Hourdin, R. Fournier, C. Hourdin, O. Talagrand, M. Collins, S. R. Lewis, P. L. Read and J. P. Hout (1999), Improved general circulation models of the Martian atmosphere from the surface to above 80 km, *J. Geophys. Res.*, *104*, 24155–24175.

- Frierson, D. M., I. M. Held, and P. Zurita-Gotor (2006), A gray-radiation aqua-planet moist GCM. part I: static stability and eddy scale, *J. Atmos. Sci.*, *63*(10), 2548–2566.
- Geen, R., F. Lambert, and G. Vallis (2018), Regime change behavior during asian monsoon onset, *J. Climate*, *31*(8), 3327–3348.
- Held, I. M. (2000), The general circulation of the atmosphere, *2000 program in geophysical fluid dynamics*.
- Held, I. M., and A. Y. Hou (1980), Nonlinear axially symmetric circulations in a nearly inviscid atmosphere, *J. Atmos. Sci.*, *37*(3), 515–533.
- Hörst, S. M. (2017), Titan’s atmosphere and climate, *J. Geophys. Res. (Planets)*, *122*(3), 432–482.
- Jennings, D. E., C. A. Nixon, R. K. Achterberg, F. M. Flasar, V. G. Kund, P. N. Romani, et al. (2016), Surface temperature on Titan during northern winter and spring, *Astrophys. J. Let.*, *816*(1), L17.
- Kang, S. M., I. M. Held, D. M. Frierson, and M. Zhao (2008), The response of the ITCZ to extratropical thermal forcing: Idealized slab-ocean experiments with a GCM, *J. Climate*, *21*(14), 3521–3532.
- Kaspi, Y., and A. P. Showman (2015), Atmospheric dynamics of terrestrial exoplanets over a wide range of orbital and atmospheric parameters, *Astrophys. J.*, *804*(1), 60.
- Korty, R. L., and T. Schneider (2008), Extent of Hadley circulations in dry atmospheres, *Geophys. Res. Lett.*, *35*(23).
- Levine, X. J., and T. Schneider (2015), Baroclinic eddies and the extent of the Hadley circulation: An idealized GCM study, *J. Atmos. Sci.*, *72*(7), 2744–2761.
- Lindzen, R. S., and A. V. Hou (1988), Hadley circulations for zonally averaged heating centered off the equator, *J. Atmos. Sci.*, *45*(17), 2416–2427.
- Linsenmeier, M., S. Pascale, and V. Lucarini (2015), Climate of earth-like planets with high obliquity and eccentric orbits: Implications for habitability conditions, *Planet. Space Sci.*, *105*, 43–59.
- Lora, J. M., J. I. Lunine and J. L. Russell (2015), GCM simulations of Titan’s middle and lower atmosphere and comparison to observations, *Icarus*, *250*, 516–528
- Merlis, T. M., T. Schneider, S. Bordoni, and I. Eisenman (2013), Hadley circulation response to orbital precession. part I: Aquaplanets, *J. Climate*, *26*(3), 740–753.

- Mitchell, J. L., and J. M. Lora (2016), The climate of Titan, *Ann. Rev. Earth Plan. Sci.*, *44*, 353–380.
- Mitchell, J. L., R. T. Pierrehumbert, D. M. Frierson, and R. Caballero (2006), The dynamics behind Titan’s methane clouds, *Proc. Natl. Acad. Sci. U.S.A.*, *103*(49), 18,421–18,426.
- Mitchell, J. L. (2008), The drying of Titan’s dunes: Titan’s methane hydrology and its impact on atmospheric circulation, *J. Geophys. Res.*, *113*, E08015
- Mitchell, J. L., R. T. Pierrehumbert, D. M. Frierson, and R. Caballero (2009), The impact of methane thermodynamics on seasonal convection and circulation in a model Titan atmosphere, *Icarus*, *203*, 250–264
- Mitchell, J. L., G. K. Vallis and S. F. Potter (2014) Effects of easonal cycle on superrotation in planetary atmospheres, *Astrophys. J.* *787*, 23
- Navarra, A., and G. Boccaletti (2002), Numerical general circulation experiments of sensitivity to Earth rotation rate, *Clim. Dyn.*, *19*(5-6), 467–483.
- Neelin, J. D., and I. M. Held (1987), Modeling tropical convergence based on the moist static energy budget, *Mon. Weath. Rev.*, *115*(1), 3–12.
- Newman, C. E., M. I. Richardson, Y. Lian and C. Lee (2016) Simulating Titans methane cycle with the TitanWRF General Circulation Model, *Icarus*, *267*, 106–134.
- Pierrehumbert, R. T. (2010), *Principles of planetary climate*, Cambridge University Press.
- Privé, N. C., and R. A. Plumb (2007), Monsoon dynamics with interactive forcing. part I: Axisymmetric studies, *J. Atmos. Sci.*, *64*(5), 1417–1430.
- Read, P. L. (2011), Dynamics and circulation regimes of terrestrial planets, *Planet. Space Sci.*, *59*(10), 900–914.
- Read, P. L. (2013), The dynamics and circulation of Venus atmosphere, in *Towards Understanding the Climate of Venus*, pp. 73–110, Springer.
- Read, P. L., S. R. Lewis, and D. P. Mulholland (2015), The physics of Martian weather and climate: a review, *Rep. Prog. Phys.*, *78*(12), 125,901.
- Roe, H. G. (2012), Titan’s methane weather, *Ann. Rev. Earth Plan. Sci.*, *40*, 355–382.
- Sánchez-Lavega, A., S. Lebonnois, T. Imamura, P. Read, and D. Luz (2017), The atmospheric dynamics of Venus, *Space Sci. Rev.*, *212*(3-4), 1541–1616.

- Schneider T., S.D.B. Graves, E.L. Schaller and M.E. Brown (2012), Polarmethane accumulation and rainstorms on Titan from simulations of the methane cycle, *Nature*, *481*, 58–61
- Turtle, E., A. Del Genio, J. Barbara, J. Perry, E. Schaller, A. McEwen, R. West, and T. Ray (2011), Seasonal changes in Titan’s meteorology, *Geophys. Res. Lett.*, *38*(3).
- Turtle, E. P., J. E. Perry, J. M. Barbara, A. D. Del Genio, S. Rodriguez, S. Le Moulic, C. Sotin, J. L. Lora, S. Faulk, P. Corlies, J. Kelland, S. M. MacKenzie, R. West, A. McEwen, J. I. Lunine, J. Pitesky, T. L. Ray, and M. Roy (2018), Titan’s Meteorology Over the Cassini Mission: Evidence for Extensive Subsurface Methane Reservoirs, *Geophys. Res. Lett.*, *45*(11)
- Walker, C. C., and T. Schneider (2005), Response of idealized hadley circulations to seasonally varying heating, *Geophys. Res. Lett.*, *32*(6).
- Walker, C. C., and T. Schneider (2006), Eddy influences on Hadley circulations: Simulations with an idealized GCM, *J. Atmos. Sci.*, *63*(12), 3333–3350.
- Wei, H. H., and S. Bordoni (2018), Energetic constrains on the ITCZ in idealized simulations with a seasonal cycle, *JAMES*, *10*(7), 1708–1725.